Viscoelastic Properties of Semiflexible Macromolecules in Solution: Brownian Dynamics Simulation of a Trumbbell Model

ARTICLE *in* MACROMOLECULES · APRIL 1994

Impact Factor: 5.8 · DOI: 10.1021/ma00097a017

2 AUTHORS:

F. Guillermo Díaz Baños
University of Murcia
47 PUBLICATIONS **472** CITATIONS
SEE PROFILE

José García de la Torre
University of Murcia
217 PUBLICATIONS **6,099** CITATIONS
SEE PROFILE

Viscoelastic Properties of Semiflexible Macromolecules in Solution: Brownian Dynamics Simulation of a Trumbbell Model

F. G. Díaz and J. García de la Torre*

Departamento de Química Física, Universidad de Murcia, 30071 Murcia, Spain

Received December 1, 1993; Revised Manuscript Received June 17, 1994®

ABSTRACT: The viscoelastic behavior of semiflexible macromolecules is studied using a trumbbell model with variable flexibility at the central hinge. The frequency-dependent solution viscosity for that model is calculated from Brownian dynamics simulations. The Green–Kubo formula is used to calculate the viscosity from flow-free Brownian trajectories. First, we obtain overall macromolecular properties such as the zero-shear intrinsic viscosity, longest relaxation times for viscoelasticity and for reorientation of the end-to-end vector, and others. We also calculate curves for the frequency dependence of the dynamic moduli. The results are compared with the existing theories of Roitman and Zimm and of Nagasaka and Yamakawa. Of particular interest is the determination of the range of flexibility for which the latter (which includes the effects of hydrodynamic interaction) is valid. Finally, we discuss the way in which hydrodynamic interaction influences the viscoelastic behavior of semiflexible macromolecules.

I. Introduction

The viscoelastic properties of macromolecules in dilute solution are very useful sources of information about the size and shape or conformation of the macromolecular solute.[1] The frequency dependence of the complex solution viscosity is determined in the case of flexible polymer chains by the intricate internal dynamics of the chain.[2] In the case of rigid particles, it is governed by the rotational dynamics of the whole body.[3] A case of particular interest is that of semiflexible macromolecules, particularly in the biological field. One class of such macromolecules is that represented by the wormlike model,[2] in which flexibility takes place all along the contour length of the chain. The classical example is DNA, although many other synthetic polymers belong to this class also. Another class is that of segmentally flexible macromolecules,[4] which are composed by a few rigid subunits joined by semiflexible joints. A variety of biopolymers, including antibodies, myosin, and others, belong to this type.

Obviously, the viscoelastic behavior of semiflexible macromolecules must be intermediate between those of flexible chains and rigid bodies. In some regard, such behavior can be expected to be a superposition of some overall rotation and a restricted internal motion. Thus in the frequency dependence curves for such macromolecules, there may be valuable information about their partial flexibility.

A very simple semiflexible model is the trumbbell, composed by two links that join three frictional, spherical elements. A potential energy opposes bending of the angle between the two links and determines the partial flexibility of the particle. Thus the trumbbell is a very simple case common to the two classes of semiflexible macromolecules described above; it is a one-swivel, two-subunit segmentally flexible particle as well as a wormlike chain with the minimum number of links. Following previous work by Hassager,[5,6] Roitman and Zimm[7] derived the viscoelastic properties of a trumbbell of arbitrary flexibility under the assumption of neglecting the hydrodynamic interaction between the frictional elements. In polymer dynamics studies, this is usually regarded as a strong approximation, but it enabled those authors a complete analytical study of the problem. With another perspective, Nagasaka and Yamakawa[8] carried out a study including hydrodynamic interaction but, in order to obtain analytical results, limited to very rigid, weakly bending trumbbells. The case of the completely flexible, freely hinged macromolecule has been considered just in terms of diffusion coefficients in previous works.[9,10]

More recently, Brownian dynamics simulation has been proposed as a useful tool to study the dynamics of semiflexible macromolecular models, and it has been particularly applied to the trumbbell model. Properties like transient electric birefringence and dichroism have been simulated for trumbbells.[11] We have also proposed how viscoelastic properties can be calculated from flow-free Brownian simulation via the Green–Kubo formalism for general models. The purpose of the present paper is to apply that procedure for the prediction of viscoelastic properties of trumbbells, checking the existing theories in the cases where they are applicable and complementing their results beyond those cases so that the effects from partial flexibility, hydrodynamic interaction, and others can be analyzed. We also consider another manifestation of the rotational and internal dynamics, namely, the end-over-end rotational diffusion,[12] so that the characteristic times of viscoelasticity and end-to-end tumbling can be compared.

II. Theory, Methods, and Model

1. Viscoelastic Properties from Brownian Dynamics Simulation. The complex frequency-dependent intrinsic viscosity $[\eta(\omega)]$ can be expressed with the Green–Kubo formula[13–17]

$$[\eta(\omega)] = \frac{N_A kT}{M\eta_0}\int_0^\infty \exp(-i\omega t)\, C(t)\, dt \qquad (1)$$

where N_A is Avogadro's number, M is the molecular weight of the polymer, η_0 is the solvent viscosity, kT is the thermal energy, and $C(t)$ is the time autocorrelation function of the xy component of the momentum flux tensor, $J^{(xy)}$, given by

$$C(t) = \langle J^{(xy)}(0)\, J^{(xy)}(t)\rangle \qquad (2)$$

* To whom correspondence should be addressed.

® Abstract published in *Advance ACS Abstracts*, August 1, 1994.

0024-9297/94/2227-5371$04.50/0

where

$$J^{(xy)} = \sum_{j=1}^{N} y_j' F_j^{(x)} \tag{3}$$

and $\langle ... \rangle$ denotes an ensemble average or, equivalently, an average over choices of the initial instant of the motion of a single particle. y_j' is the y coordinate of the ith polymer element in a reference system of coordinates centered in a hydrodynamic center, C, which, for a model with identical beads is assumed to be the center of mass. In eq 3, $F_j^{(x)}$ is the x component of the total force due to external fields (which are not present in our problem) and internal constraints but does not include frictional terms.

For our purposes it is convenient to separate the real and the imaginary parts of the viscosity, which are denoted as η' and η'', so that $[\eta(\omega)] = [\eta'(\omega)] - i[\eta''(\omega)]$. The magnitudes usually measured experimentally are the storage and loss moduli, which can be defined as[18] $[G'(\omega)] = [\eta''(\omega)]\omega$ and $[G''(\omega)] = [\eta'(\omega)]\omega$.

We assume that $C(t)$ can be represented by a series of exponentials:

$$C(t) = \sum_m a_m e^{-t/\tau_m} \tag{4}$$

This may be indeed a theoretical result, as in the Rouse–Zimm model[2] for flexible chains and in the Roitman–Zimm[7] study of the trumbbell. Otherwise, eq 4 can be regarded as a valid fitting expression that describes well a set of simulated $C(t)$ data. From eq 4, the relaxation moduli are given by

$$[G'(\omega)] = \frac{N_A kT}{M\eta_0} \sum_{m=1} \frac{a_m \tau_m^2 \omega^2}{1 + (\tau_m \omega)^2} \tag{5a}$$

$$[G''(\omega)] = \frac{N_A kT}{M\eta_0} \sum_{m=1} \frac{a_m \tau_m \omega}{1 + (\tau_m \omega)^2} \tag{5b}$$

A relevant particular case is $\omega = 0$. From former equations we obtain the intrinsic viscosity.

$$[\eta(0)] = \frac{N_A kT}{M\eta_0} \int_0^\infty C(t)\, dt = \frac{N_A kT}{M\eta_0} \sum_{m=1} a_m \tau_m \tag{6}$$

The zero-frequency intrinsic viscosity determines the part of the loss modulus $[G''(\omega)]$ curves corresponding to frequencies lower than the reciprocal of the longest relaxation time. Indeed, from eqs 5b and 6, it turns out that

$$[G''(\omega)] = [\eta(0)]\omega \quad (\omega \ll \tau_1^{-1}) \tag{7}$$

In the same region, the frequency dependence of the storage modulus $[G'(\omega)]$ can be expressed in terms of a single numerical value, which is sometimes called the second Rivlin–Eriksen coefficient a_2':

$$[G'(\omega)] = a_2'\omega^2 \quad (\omega \ll \tau_1^{-1}) \tag{8}$$

where we have from eqs 5a and 8 that

$$a_2' = \frac{N_A kT}{M\eta_0} \sum_{m=1} a_m \tau_m^2 \tag{9}$$

The region where eqs 7 and 8 hold is a large part (several decades) of the experimentally assessible region.

In this work the evaluation of the time correlation functions is based in the analysis of trajectories of the polymer model that are generated simulating its Brownian dynamics. We use a simulation procedure based on the algorithm of Ermak and McCammon.[19] Basically, if $\mathbf{r}_i^\circ$ is the position vector of bead i, the position after a time step Δt is given by

$$\mathbf{r}_i = \mathbf{r}_i^\circ + \frac{\Delta t}{kT} \sum_j \mathbf{D}_{ij}^\circ \mathbf{F}_j + \mathbf{R}_i(\Delta t) \tag{10}$$

where $\mathbf{D}_{ij}^\circ$ is the ij block of the diffusion tensor, whose value depends on how hydrodynamic interaction (HI) is described. The tensor we have used to include this effect is that of Rotne, Prager, and Yamakawa.[20,21] $\mathbf{R}_i$ is a random vector with a Gaussian distribution having a zero mean and a covariance equal to $\langle \mathbf{R}_i \mathbf{R}_j \rangle = 2\, \mathbf{D}_{ij}^\circ \Delta t$. Actually, instead of eq 10 we use a second-order modification that is computationally more effective.[22]

2. Trumbbell Model: Description, Properties, and Existing Theories. The model we are going to use is the so-called trumbbell. It is composed by three identical beads joined by two quasirigid bonds. A restoring potential $V/kT = Q\alpha^2$ opposes bending angle α, with Q a stiffness parameter. For $Q = 0$ we have a completely flexible hinged trumbbell, while the $Q \to \infty$ limit corresponds to a completely rigid, straight trumbbell. In numerical work we take $Q = 50$ as a sufficiently high value to represent this limit. The bonds are stiff springs with equilibrium length b and a spring constant such that the mean squared length is $1.05b^2$. Previous Brownian dynamics simulation studies have been reported by these authors[12,23] where more details about this model can be found.

Using the rigid-body treatment[24] (RBT) the dynamics of segmentally flexible macromolecules can be approached from the well-developed theory of rigid particles evaluating properties as averages of values obtained for the possible conformations, which are regarded as instantaneously rigid. Conformations can be generated in a variety of ways and from them it is straightforward to calculate values of observable parameters like the intrinsic viscosity and the longest relaxation time. In this work, the procedure we have used to generate the different conformations has been a Brownian dynamics simulation. For the rigid body calculations, the Rotne–Prager–Yamakawa hydrodynamic tensor has been used. In the case of rotational relaxation times, averages have to be treated carefully.[25,26]

Previous works[5-8] have shown that the viscoelastic behavior of semiflexible particles is the result of two main contributions: a slow relaxation which is nearly pure rotation and a fast mixed bend–rotation relaxation. This means that at least the longest relaxation time obtained for viscoelasticity may be comparable to that obtained for rotational dynamics. The rotational dynamics can be characterized by means of correlation functions related to the reorientation of a certain unitary vector fixed to the particle **A**. If θ_A is the angle formed by an initial orientation of **A** and this vector after time t, then $\cos\theta_A(t) = \mathbf{A}(t)\cdot\mathbf{A}(0)$. One very useful correlation function is that associated with the second Legendre polynomial $\langle P_2[\cos\theta_A(t)] \rangle$. Among the possible choices for **A** the most suitable vector to characterize the overall rotational behavior is the end-to-end vector.

In the Roitman–Zimm (RZ) theory,[7] $[G'(\omega)]$ is of the same form as eq 5a. $[G''(\omega)]$ is a sum of terms like in eq 5b plus a term linear in ω, which does not appear in our

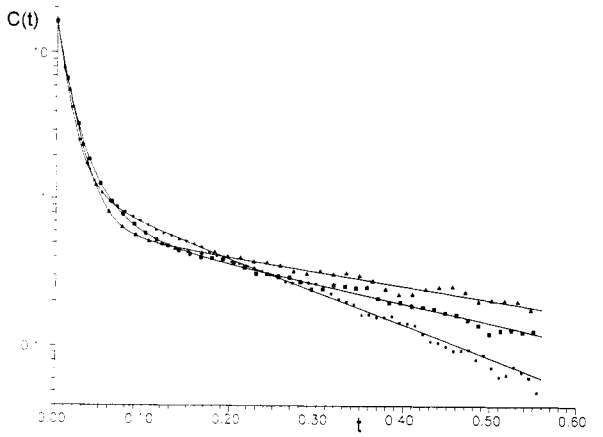

Figure 1. Time correlation functions, $C(t)$, as defined in eqs 2 and 3, calculated from Brownian trajectories for various values of the rigidity parameter: (*) $Q = 0$; (■), $Q = 1$; (▲), $Q = 50$. Solid lines represent the fitting multiexponential curves.

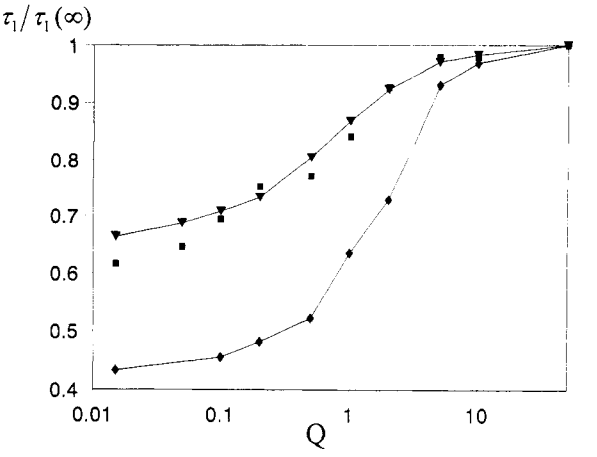

Figure 2. Longest relaxation time normalized to the value of the rigid, straight particle. All the results are for the HI case. $\tau_1(\infty) \equiv \tau_1(Q = 50)$. (▼) RBT; (♦) GKC; (■) REE.

treatment. The reason for the difference is the nature of the bonds in the trumbbell, which are absolutely rigid in the RZ theory, while they have a residual flexibility in our model. As a consequence, at very high frequencies, $[G''(\omega)] \propto \omega$ in the RZ treatment, while we will find $[G''(\omega)] \propto \omega^{-1}$ in our simulations. This difference has already been noticed by comparison of rigid and stiff dumbbells.[16,23] The RZ values for the τ_m's and a_m's are listed in Table V of ref 7. As in any model in which hydrodynamic interaction is neglected, the zero-frequency viscosity turns out to be proportional to the squared radius of gyration.

We will also compare our results with the Nagasaka–Yamakawa (NY) theory,[8] valid for high rigidity constant Q. These authors express $[G'(\omega)]$ and $[G''(\omega)]$ as a sum of the type of eq 5a but with only two terms with relaxation times τ_1 and τ_2 for which these authors provide analytical expressions. The loss moduli include a term proportional to ω as in the RZ results, since the model is the same. These authors also give an explicit expression for $[\eta(0)]$.

III. Results

We first point out that the results are given as dimensionless quantities (denoted with asterisks) that are obtained dividing by the following factors: length, b (which is the characteristic bond length in the polymer model); time, $\zeta b^2/kT$, where ζ is the friction coefficient $\zeta = 6\pi\eta_0\sigma$, identical for all the spheres; frequency (inverse of the time), $kT/\zeta b^2$; forces, kT/b; and finally the intrinsic viscosity, $N_A\zeta b^2/\eta_0 M$. As a consequence of these definitions, the reduced values for the storage and loss moduli are obtained dividing by $N_A kT/\eta_0 M$.

In this work simulations were run for a wide range of flexibility from practically rigid ($Q = 50$) to completely flexible ($Q = 0$). To obtain accurate enough results for the Green–Kubo correlation data (discrete version of $C(t)$), they had to be obtained from the average of 20 simulations of 10 million steps each (no HI) and 5 million steps (HI). The step length was $\Delta t^* = 0.0002$. Multiexponential fits have been done using the DISCRETE[27,28] program from $t^* = 0$ to $t^* = 0.56$. Some examples of the resulting $C(t)$ and the fitting curves are displayed in Figure 1. One of the main features of this program is that no *a priori* information is required about the number of exponentials or estimates of parameters. In the case of the rigid body treatment we have done two different simulations of 5×10^5 steps each ($\Delta t^* = 0.0002$) for both the HI and the no-HI cases. Only one in ten of the conformations has been considered for the averages of the intrinsic viscosity. Regarding the study of the rotational dynamics correlation function, we have carried out for each case four simulations of 5×10^5 steps each ($\Delta t^* = 0.0002$). Both cases, with HI (Rotne–Prager–Yamakawa) and without HI, have been studied. $\langle P_2 \rangle$ for the end-to-end vector appears like a multiexponential curve which has been fitted using DISCRETE.

The results for the overall (single-valued) properties are listed in Table 1. We analyze first the validity of the rigid body treatment for these properties. It is evident that the RBT values for the intrinsic viscosity are very good when compared to simulations and other theories. This is so regardless of whether HI is neglected or included. Thus, the effects of the approximations embodied in that treatment are negligible in this property. We hope that the situation should be the same for other, more realistic semiflexible models such as the weakly bending rod. Analyzing similarly the values for the longest relaxation time, τ_1, we note that the RBT values in the no-HI case are close to all other comparable values, with a systematic deviation downward that is more noticeable in the flexible limit. However, when hydrodynamic interaction is included (as it should be), a more clear tendency shows up: the RBT τ_1 values are practically coincident with the longest relaxation time for reorientation of the end-to-end vector; however, they are clearly different from the longest viscoelastic relaxation times obtained either from our simulations or from the Nagasaka–Yamakawa theory. This is clearly illustrated in Figure 2, where the values are normalized to the most rigid case to eliminate in the comparison possible residual effects. This situation suggests an interesting conclusion: although some theories predict that a unique spectrum of relaxation times may describe various dynamic properties, when HI is included and the dynamics is described from first principles (as in BD simulation), that may not be true. Particularly the observed or apparent longest relaxation time may be different from one property to another.

Our simulation results without HI can be used to test the Roitman–Zimm theory.[7] The comparison of the numerical results of the single-valued properties can be made from the data in Table 1, and the curves obtained for the two dynamic moduli are compared in Figure 3. We find that the RZ theory gives very good values for $[\eta(0)]$. The longest relaxation time is also accurately predicted, except perhaps for the most flexible trumbbell, when the deviation is 15% at most. For the a_2' coefficient, the

Table 1. Radius of Gyration, Intrinsic Viscosity, Inverse of the Longest Relation Time, and Second Rivlin–Eriksen Expansion Coefficient Obtained for Different Values of Flexibility from Different Methods

		no HI					HI			
Q	$\langle S^2\rangle^a$	RZ[b]	NY[c]	RBT[d]	GKC[e]	REE[f]	NY	RBT	GKC	REE
					$[\eta(0)]^*$					
0	0.473	0.237		0.237	0.244			0.407	0.389	
0.05	0.486	0.243		0.243				0.415		
0.1	0.491	0.246		0.245	0.252			0.422	0.393	
0.2	0.516	0.258		0.258	0.266			0.429	0.410	
0.5	0.571	0.286	0.263	0.286	0.293		0.909	0.449	0.443	
1.0	0.614	0.307	0.299	0.207	0.326		0.691	0.462	0.451	
2.0	0.648	0.324	0.323	0.324	0.339		0.586	0.469	0.449	
5.0	0.676	0.338	0.339	0.338	0.350		0.523	0.473	0.480	
10	0.688	0.344	0.344	0.344	0.347		0.503	0.474	0.483	
50	0.699	0.349	0.349	0.349	0.338		0.487	0.485	0.492	
					τ_1^{*-1}					
0		5.44		4.69	5.16	5.21		3.51	5.10	3.80
0.05				4.54		5.23		3.39		3.62
0.1				4.47	4.84	4.92		3.29	4.86	3.37
0.2				4.22	4.58	4.72		3.18	4.59	3.11
0.5		4.18	5.14	3.71	4.11	4.03		2.89	4.23	3.03
1.0		3.67	3.79	3.38	3.26	3.68		2.68	3.48	2.78
2.0		3.34	3.35	3.15	3.25	3.24		2.52	3.03	2.52
5.0			3.13	2.95	3.05	3.07		2.40	2.37	2.39
10			3.06	2.92	3.07	3.00		2.37	2.28	2.39
50		3.00	3.01	2.87	2.96	2.94	2.45	2.33	2.21	2.34
					$a_2'^* \times 10^2$					
0		2.17			2.48				4.37	
0.05										
0.1					2.81				4.47	
0.2					3.23				4.84	
0.5		3.61	4.26		4.04		6.16		5.59	
1.0		4.55	4.33		5.78		6.76		6.76	
2.0		5.43	5.31		6.15		8.26		7.52	
5.0			6.24		7.02		9.56		11.21	
10			6.60		6.93		10.07		11.87	
50		6.99	6.92		6.86		10.05		12.82	

[a] Average over conformations generated in the BD simulation. [b] RZ: Roitman and Zimm. For $[\eta(0)]$ value obtained as $\langle S^2\rangle/2$. [c] NY: Nagasaka and Yamakawa.[8] [d] RBT: Rigid body treatment. [e] GKC: Green–Kubo correlation function from Brownian dynamics. [f] REE: Rotational dynamics correlation function (P_2) for end-to-end vector.

agreement is not so good; there is a systematic deviation of 15–20% throughout the whole range of Q.

In Figure 3A we see that good agreement between our curves for $[G'(\omega)]$ and those of RZ up to moderate frequencies (while the behavior is linear) is obtained. In the intermediate range of frequencies the accordance is lost, and for high frequencies we find curves tending to a limiting value independent of the flexibility, while those of RZ are dependent on this property. The reason is clear: according to eq 5a, when $\omega \to \infty$, $[G'(\omega)] \to C(0)$, which is practically the same for all cases of flexibility. A magnitude comparable with $C(0)$ from the point of view of RZ is nonsense. We cannot forget either that models used in both cases are different with total rigidity in bonds for RZ and a residual stretching flexibility in this work. In fact, we studied marginally this aspect, finding a clear dependence of the value of $[G'(\infty)]$ on the connector spring constant for our model (results not shown). The comparison between our no-HI simulation results and the RZ values in the case of $[G''(\omega)]$ is presented in Figure 3B. The accordance is good in the low-frequency region since this part of the diagram is determined by $[\eta(0)]$, which, as described above, is well predicted by the RZ theory. The qualitative disagreement observed in the high-frequency region is due again to the difference between the two models. In this case the explanation is even clearer: the solution of the Kirkwood equation obtained by Hassager[6] and used by RZ gives a term proportional to ω for the loss modulus (see eq 5.2 of ref 7) that is determining the behavior at high frequencies and that has no parallel in eq 5b.

Our simulation results can also be compared with the Nagasaka–Yamakawa theory for highly rigid trumbbells with HI (the NY equations can also be particularized for the no-HI case). Looking again at Table 1, we see how the NY numerical values are very close to their HI or no-HI counterparts from the rigid limit down to a value or the rigidity parameter of about $Q = 1.0$–0.5, depending on the property (in Table 1 NY values are not reported for low Q, when they deviate remarkably from simulation or RZ values). This is so for the three properties listed in the no-HI case. In the HI case there is agreement for τ_1 and a_2 and for $[\eta(0)]$ in the $Q \to \infty$ limit. For $[\eta(0)]$ at not too large Q (results not listed) we have found an anomalous behavior of the NY values: $[\eta(0)]$ increases with decreasing Q (increasing flexibility) instead of decreasing as it should. This can be clearly verified by simple numerical evaluation of eqs 48 ($\omega = 0$), 50, and 51 in the NY paper.[8] We ignore the origin of this defect of the NY theory.

The NY curves for $[G'(\omega)]$ and $[G''(\omega)]$ in the most relevant case that includes HI are compared with our HI simulation results in Figure 4 (NY curves are presented only for $Q = 50$ and $Q = 1$, since the theory is not valid for $Q = 0$). In $[G'(\omega)]$, the agreement is acceptable for low frequencies, as determined by the fair agreement between the a_2' values. For high frequencies the origin of the discrepancy is the above-commented difference in the storage behavior of the connectors in the models, although

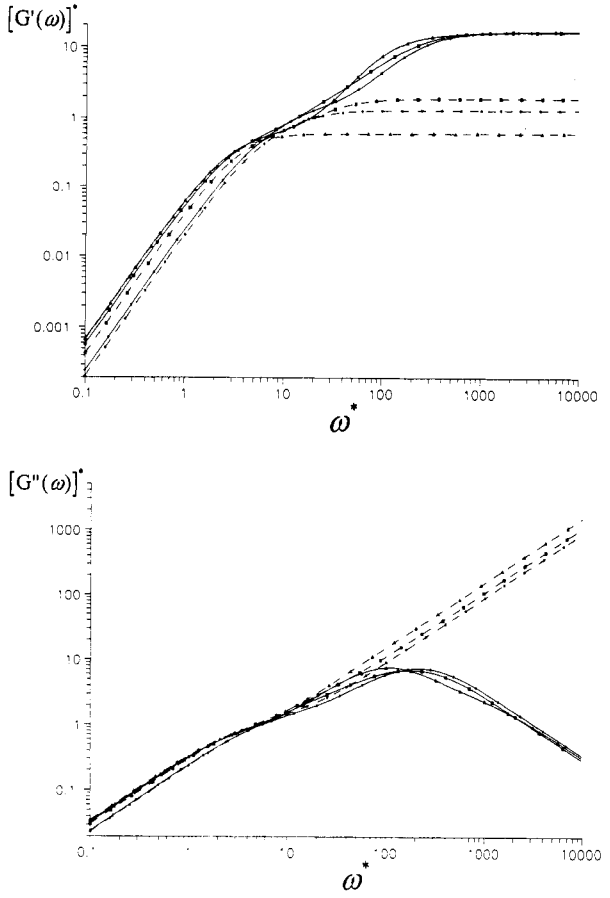

Figure 3. Dynamic moduli $[G'(\omega)]^*$ (A, top) and $[G''(\omega)]^*$ (B, bottom) vs ω^* for trumbbells without HI with $Q = 0$ (*), 1 (■), and 50 (▲) (symbols are used just to distinguish different Q). The continuous curves correspond to the simulation results, and the dashed curves are calculated from the Roitman–Zimm theory.

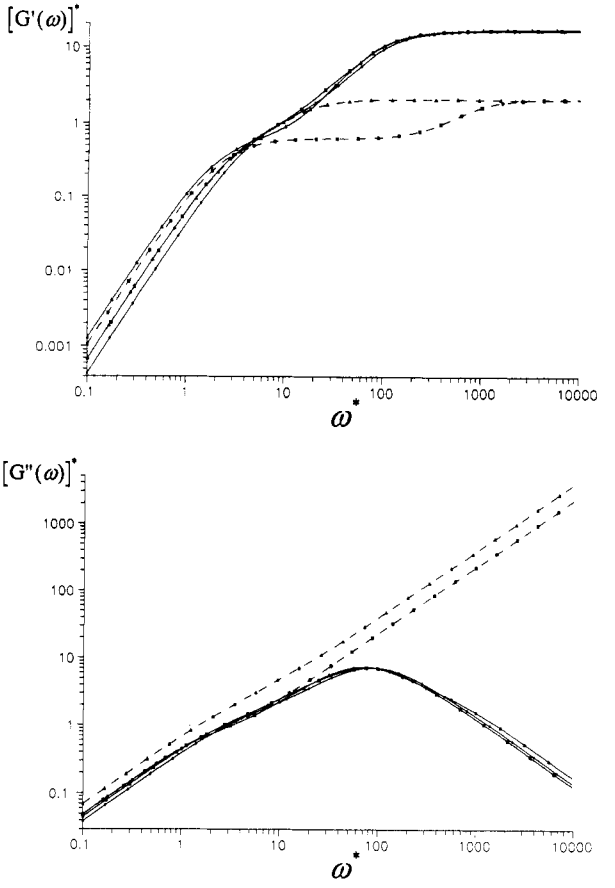

Figure 4. Dynamic moduli $[G'(\omega)]^*$ (A, top) and $[G''(\omega)]^*$ (B, bottom) vs ω^* for trumbbells with HI with $Q = 0$ (*), 1 (■), and 50 (▲) (symbols are used just to distinguish different Q). The continuous curves correspond to the simulation results, and the dashed curves are calculated from the Nagasaka–Yamakawa theory ($Q = 0$ is omitted in the latter case because the theory is not valid for the flexible limit).

it is to be noted that the deviation is already remarkable at moderate, intermediate frequencies (say $10 \leq \omega^* < 100$). It is not clear to what extent the deviation in this region is due to differences in the model or to particularities in the NY treatment. For the loss modulus, $[G''(\omega)]$, when $Q = 50$ the agreement is very good at low ω, and the divergence begins by $\omega^* \cong 100$. In the intermediate region $10 < \omega^* < 100$ the agreement is now semiquantitative, and therefore the discrepancy noted for $[G'(\omega)]$ in this region may be significantly model independent. The NY curve for $Q = 1$ is affected by the defect commented above.

Finally, in Figure 5 we compare simulation results with our model (thus eliminating any model dependence) both with and without HI. For the sake of clarity in the diagrams, only curves for a semiflexible trumbbell with $Q = 1$ are plotted. It is evident that HI has a quantitative effect in both moduli. However, the shapes of the HI and no-HI curves are quite similar. Indeed, if a reduced frequency defined in terms of the intrinsic viscosity as $\omega_F = \omega^*[\eta(0)]$ (which is commonly employed to plot experimental data) is used instead of ω^* in the diagrams, the HI and no-HI curves come even closer to each other.

In an attempt to go beyond the simple trumbbell model, we tried the simulations for longer semiflexible chains. Actually, we carried out calculations for $N = 11$, finding that the number of time steps required to obtain reproducible results should be of the same order as that for the trumbbell but the number of beads is nearly 4 times larger. In addition, the computer time grows as N^3 in the case with HI. Both aspects imply a very large increase in computer power that was out of our reach. While this can

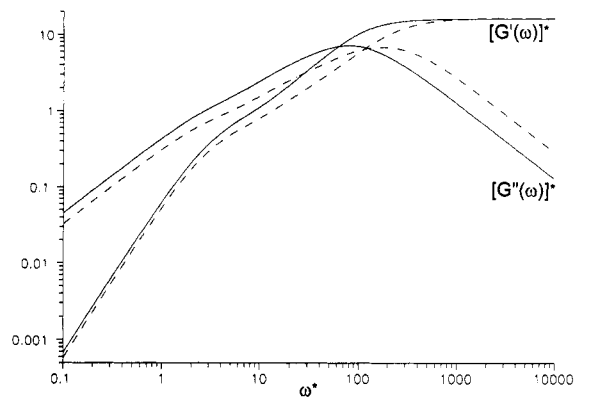

Figure 5. Dynamic moduli $[G'(\omega)]^*$ and $[G''(\omega)]^*$ vs ω^* for trumbbells with HI (continuous curves) and without HI (dashed curves) for $Q = 1$.

be achieved hopefully in the near future, the general conclusions drawn from the trumbbell model can be used as representative of the behavior of semiflexible chains.

IV. Conclusions

We have shown how the viscoelastic behavior of semiflexible macromolecules can be studied by Brownian dynamics simulation by means of a Green–Kubo expression involving an autocorrelation function that can be calculated from Brownian trajectories in the absence of flow. Although numerical difficulties restrict the analysis to models with few frictional elements, we have been able

to study in detail the trumbbell model, for which the theoretical predictions of Roitman and Zimm (without HI) and Nagasaka and Yamakawa (with HI, high Q) are available. The RZ predictions at low frequency are confirmed by our simulation, while at high frequencies there is a discrepancy arising from the different type of connectors in the models. At low frequencies, the agreement between our simulations and the NY theory with HI is very good from the rigid limit down to values of the rigidity constant of about $Q \cong 0.5$–1.0. This conclusion determines the range of validity of that theory. Comparison of simulations with and without HI indicates that HI has an important quantitative effect that is somehow uniform through the whole accessible range of frequencies but does not affect remarkably the shape of the viscoelastic curves.

Acknowledgment. This work was supported by Grant PB90-0303 from the Comisión Asesora de Investigación Científica y Técnica.

References and Notes

(1) Ferry, J. D. *Viscoelastic Properties of Polymers*; Wiley: New York, 1970.
(2) Yamakawa, H. *Modern Theory of Polymer Solutions*; Harper and Row: New York, 1971.
(3) Wegener, W. A. *Biopolymers* **1984**, *23*, 2234.
(4) Yguerabide, J.; Epstein, H. F.; Stryer, L. *J. Mol. Biol.* **1970**, *51*, 573.
(5) Hassager, O. *J. Chem. Phys.* **1974**, *20*, 2111.
(6) Hassager, O. *J. Chem. Phys.* **1974**, *20*, 4001.
(7) Roitman, D.; Zimm, B. H. *J. Chem. Phys.* **1984**, *81*, 6333.
(8) Nagasaka, K.; Yamakawa, H. *J. Chem. Phys.* **1985**, *83*, 6480.
(9) Harvey, S. C.; Mellado, P.; García de la Torre, J. *J. Chem. Phys.* **1983**, *78*, 2081.
(10) García de la Torre, J.; Mellado, P.; Rodes, V. *Biopolymers* **1985**, *24*, 2145.
(11) Lewis, R. J.; Allison, S. A.; Eden, D.; Pecora, R. *J. Chem. Phys.* **1988**, *89*, 2490.
(12) Díaz, F. G.; García de la Torre, J. *J. Chem. Phys.* **1988**, *88*, 7698.
(13) Stockmayer, W. H.; Gobush, W.; Chikahisa, Y.; Carpenter, D. K. *Faraday Discuss. Chem. Soc.* **1970**, *49*, 182.
(14) Yamakawa, H.; Tanaka, G.; Stockmayer, W. H. *J. Chem. Phys.* **1974**, *61*, 435.
(15) Felderhof, B. H.; Deutch, J. M.; Titulaer, U. M. *J. Chem. Phys.* **1975**, *63*, 740.
(16) Wilemski, G. J. *J. Chem. Phys.* **1984**, *81*, 6106.
(17) Jagannathan, A.; Oono, Y.; Schaub, B. *J. Chem. Phys.* **1986**, *86*, 2276.
(18) Bird, R. B.; Hassager, O.; Armstrong, R. C.; Curtiss, C. F. *Dynamics of Polymeric Liquids*; Wiley: New York, 1977.
(19) Ermak, D. L.; McCammon, J. A. *J. Chem. Phys.* **1978**, *69*, 1352.
(20) Rotne, J.; Prager, S. *J. Chem. Phys.* **1969**, *50*, 4381.
(21) Yamakawa, H. *J. Chem. Phys.* **1970**, *53*, 436.
(22) Iniesta, A.; García de la Torre, J. *J. Chem. Phys.* **1990**, *92*, 2015.
(23) Díaz, F. G.; García de la Torre, J.; Freire, J. J. *Macromolecules* **1990**, *23*, 3144.
(24) García de la Torre, J.; Bloomfield, V. A. *Q. Rev. Biophys.* **1981**, *14*, 81.
(25) Iniesta, A.; Díaz, F. G.; García de la Torre, J. *Biophys. J.* **1988**, *54*, 269.
(26) Hagerman, P.; Zimm, B. H. *Biopolymers* **1982**, *20*, 1481.
(27) Provencher, S. *J. Chem. Phys.* **1976**, *64*, 2772.
(28) Provencher, S. *Biophys. J.* **1976**, *16*, 27.